BIOCHEMISTRY
including biophysical chemistry & molecular biology

Article

pubs.acs.org/biochemistry

The PH Domain of Phosphoinositide-Dependent Kinase-1 Exhibits a Novel, Phospho-Regulated Monomer−Dimer Equilibrium with Important Implications for Kinase Domain Activation: Single-Molecule and Ensemble Studies

Brian P. Ziemba,[†] Carissa Pilling,[†] Véronique Calleja,[‡] Banafshé Larijani,[‡] and Joseph J. Falke*[,†]

[†]Department of Chemistry and Biochemistry and Molecular Biophysics Program, University of Colorado, Boulder, Colorado 80309-0596, United States

[‡]Cell Biophysics Laboratory, Cancer Research U.K., Lincoln's Inn Fields Laboratories, London Research Institute, London WC2A 3LY, U.K.

ABSTRACT: Phosphoinositide-dependent kinase-1 (PDK1) is an essential master kinase recruited to the plasma membrane by the binding of its C-terminal PH domain to the signaling lipid phosphatidylinositol-3,4,5-trisphosphate (PIP_3). Membrane binding leads to PDK1 phospho-activation, but despite the central role of PDK1 in signaling and cancer biology, this activation mechanism remains poorly understood. PDK1 has been shown to exist as a dimer in cells, and one crystal structure of its isolated PH domain exhibits a putative dimer interface. It has been proposed that phosphorylation of PH domain residue T513 (or the phosphomimetic T513E mutation) may regulate a novel PH domain dimer−monomer equilibrium, thereby converting an inactive PDK1 dimer to an active monomer. However, the oligomeric states of the PH domain on the membrane have not yet been determined, nor whether a negative charge at position 513 is sufficient to regulate its oligomeric state. This study investigates the binding of purified wild-type (WT) and T513E PDK1 PH domains to lipid bilayers containing the PIP_3 target lipid, using both single-molecule and ensemble measurements. Single-molecule analysis of the brightness of the fluorescent PH domain shows that the PIP_3-bound WT PH domain on membranes is predominantly dimeric while the PIP_3-bound T513E PH domain is monomeric, demonstrating that negative charge at the T513 position is sufficient to dissociate the PH domain dimer and is thus likely to play a central role in PDK1 monomerization and activation. Single-molecule analysis of two-dimensional (2D) diffusion of PH domain−PIP_3 complexes reveals that the dimeric WT PH domain diffuses at the same rate as a single lipid molecule, indicating that only one of its two PIP_3 binding sites is occupied and there is little penetration of the protein into the bilayer as observed for other PH domains. The 2D diffusion of T513E PH domain is slower, suggesting the negative charge disrupts local structure in a way that allows deeper insertion of the protein into the viscous bilayer, thereby increasing the diffusional friction. Ensemble measurements of PH domain affinity for PIP_3 on plasma membrane-like bilayers reveal that the dimeric WT PH domain possesses a one order of magnitude higher target membrane affinity than the previously characterized monomeric PH domains, consistent with a dimerization-triggered, allosterically enhanced affinity for one PIP_3 molecule (a much larger affinity enhancement would be expected for dimerization-triggered binding to two PIP_3 molecules). The monomeric T513E PDK1 PH domain, like other monomeric PH domains, exhibits a PIP_3 affinity and bound state lifetime that are each 1 order of magnitude lower than those of the dimeric WT PH domain, which is predicted to facilitate release of activated, monomeric PDK1 to the cytoplasm. Overall, the study yields the first molecular picture of PH domain regulation via electrostatic control of dimer−monomer conversion.

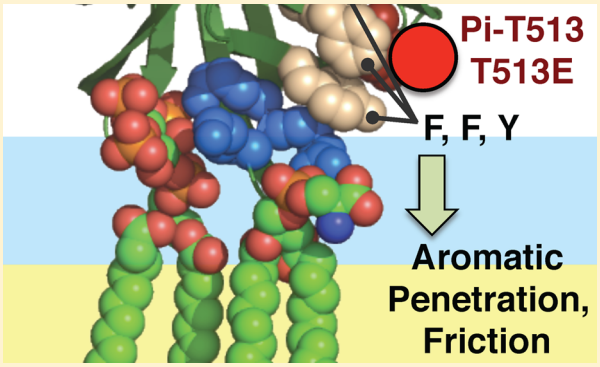

Phosphoinositide-dependent kinase-1 (PDK1) possesses an N-terminal Ser/Thr kinase domain and a C-terminal PIP_3-specific PH domain that recruits the kinase to the plasma membrane during PIP_3 signaling. The membrane-bound kinase is proposed to self-activate via an autophosphorylation reaction that results in phosphorylation of activation loop residue S241 and of PH domain residues S410 and T513.[1,2] Subsequently, the active PDK1 kinase can phospho-activate plasma membrane targets such as corecruited protein kinase B (also known as AKT1) or can dissociate from the membrane and phosphorylate cytoplasmic targets, including classical protein kinase C isoforms (cPKCs).[2−5] In short, PDK1 is a master kinase that regulates an array of pathways and processes ranging from actin remodeling in cell migration to cell proliferation and inhibition

Received: April 18, 2013
Revised: May 18, 2013
Published: June 8, 2013

dx.doi.org/10.1021/bi400488f | *Biochemistry* 2013, 52, 4820−4829

of apoptosis in pathways that control cell growth and survival.[2−4,6−12] Notably, PDK1 in concert with PI3Ka and AKT1 forms the infamous PI3Ka/PDK1/AKT1 oncogenic triad linked to human cancers and other diseases.[11,13−15] PDK1 overexpression or overstimulation is observed in a significant proportion of human cancers, especially breast cancer.[14] Thus, PDK1 is a current target for inhibitor development, and a molecular understanding of its activation mechanism could facilitate those efforts, potentially yielding new cancer therapies.[13,16]

Live cell studies of intact PDK1, fragments, and mutants have provided evidence that inactive PDK1 in the cytoplasm is a homodimer and have suggested that monomeric PDK1 is the more active form.[2] For example, full-length wild-type (WT) PDK1 and the T513E mutant have been compared in cells, and the greater kinase activity of the mutant is hypothesized to arise from its conversion to the monomer.[2] However, the mechanism of dimer-to-monomer conversion is not well understood, including the role of the PH domain in this mechanism, and phospho- or phospho-mimetic regulation of the isolated PH domain oligomeric state has not been previously described.[17−20] One crystal structure of the isolated PDK1 PH domain shows a putative dimer; however, the observed geometry would prevent both PH domains from simultaneously binding their target PIP_3 lipids [Protein Data Bank (PDB) entry 1W1H[21]], while another crystal structure of the same domain is not dimeric (PDB entry 1W1D[21]). In short, the existing PDK1 data[1−5,21] cannot fully resolve the three different models of PH domain−membrane interaction illustrated in Figure 1. In model 1, the dimeric PH domain docks to the target plasma membrane but, as suggested by the structure of the crystallographic dimer, is sterically constrained to bind only one PIP_3 lipid. Subsequent phosphorylation of T513 triggers the dissociation of the dimer, yielding two monomeric PH domains that each bind a single PIP_3 lipid. In model 2, the dimeric PH domain undergoes a structural rearrangement upon membrane docking that allows the dimer to simultaneously bind two PIP_3 lipids, until the phosphorylation of T513 triggers the dissociation of the dimer into two monomeric PH domains each bound to a single PIP_3 lipid. In model 3, the dimeric PH domain spontaneously dissociates into monomers upon membrane binding, such that the primary function of T513 phosphorylation is not to regulate PH domain dimer−monomer conversion but, instead, to regulate the kinase domain oligomeric state or activity by an allosteric signal. To resolve these models, it is essential to conduct studies of the isolated WT and phospho-mimetic T513E PH domains under carefully controlled conditions.

This study employs single-molecule and ensemble methods to determine the oligomeric states, membrane contacts, and target membrane affinities of the isolated WT and T513E PDK1 PH domains. The results provide strong evidence against models 2 and 3 while supporting and refining model 1. Furthermore, the findings provide new insights into the target membrane affinities and protein−bilayer contacts of both the homodimeric and monomeric states of the PDK1 PH domain. Finally, the results suggest a molecular model for the mechanism by which phosphorylation regulates a PH domain dimer-to-monomer conversion proposed to regulate the kinase activity of full-length PDK1.

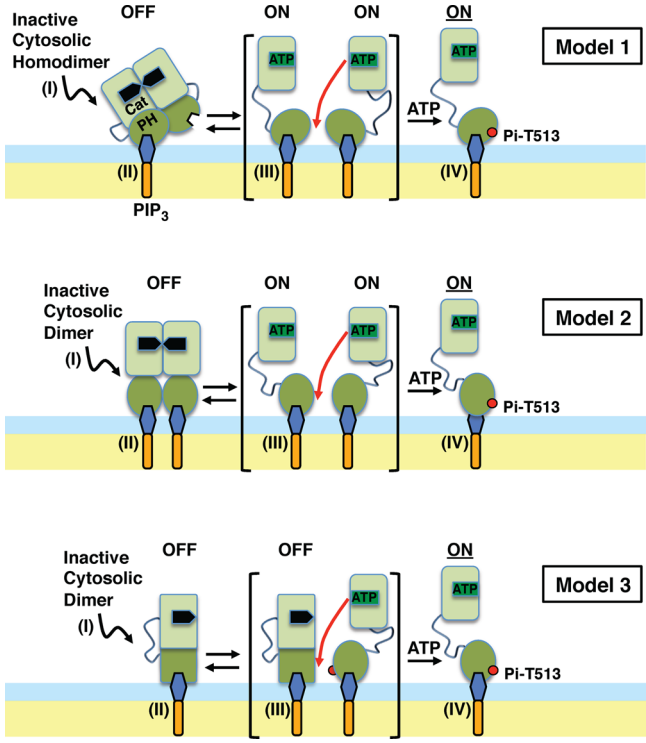

Figure 1. Schematic view of three alternative models of PDK1 activation. Shown is PDK1 docking to the exposed leaflet of a bilayer (headgroup layer colored light blue, hydrocarbon core colored pale yellow) where it binds its target lipid, PIP_3. In model 1, the dimeric PH domain docks to the target plasma membrane but, as suggested by the structure of the crystallographic dimer (PDB entry 1W1H[21]), is sterically constrained to bind only one PIP_3 lipid until the phosphorylation of T513 triggers the dissociation of the dimer yielding two monomeric PH domains that each bind a single PIP_3 lipid.[2] In model 2, the dimeric PH domain undergoes a structural rearrangement upon membrane docking that allows the dimer to simultaneously bind two PIP_3 lipids, until the phosphorylation of T513 triggers the dissociation of the dimer into two monomeric PH domains each bound to a single PIP_3.[2] In model 3, the dimeric PH domain spontaneously dissociates into monomers upon membrane binding and the phosphorylation of T513 does not regulate dimer−monomer conversion but instead activates the kinase domain by an allosteric conformational signal. The PH domain image is based on the crystal structure of PDB entry 1W1H,[21] and the kinase domain image is based on the crystal structure of PDB entry 1H1W.[36]

MATERIALS AND METHODS

Reagents. All lipids were synthetic unless otherwise indicated. DO (18:1, 18:1) lipids were used for single-molecule measurements in model membranes as described previously.[22,23] 1,2-Dioleoyl-*sn*-glycero-3-phosphocholine (DOPC, PC), 1,2-dioleoyl-*sn*-glycero-3-phospho-L-serine (DOPS, PS), and 1,2-dioleoyl-*sn*-glycero-3-phosphoinositol 3,4,5-trisphosphate [DOPI(3,4,5)P3, PI(3,4,5)P3] were from Avanti Polar Lipids. PO (16:0, 18:1) lipids, $DPPIP_3$ (saturated), natural lipids, and a fluorescent lipid were used for ensemble measurements in plasma membrane-like membranes as described previously.[24,25] 1-Palmitoyl-2-oleoyl-*sn*-glycero-3-phosphocholine (phosphatidylcholine, POPC, or PC), 1-palmitoyl-2-oleoyl-*sn*-glycero-3-phosphoethanolamine (phosphatidylethanolamine, POPE, or PE), 1-palmitoyl-2-oleoyl-*sn*-glycero-3-phosphoserine (phosphatidylserine, POPS, or PS), natural L-α-phosphatidylinositol (PI) from bovine liver, and

dx.doi.org/10.1021/bi400488f | *Biochemistry* 2013, 52, 4820−4829

natural sphingomyelin (SM) from porcine brain were from Avanti Polar Lipids, while 1,2-dipalmitoylphosphatidylinositol 3,4,5-trisphosphate [phosphatidylinositol 3,4,5-trisphosphate, PI(3,4,5)P_3, or PIP_3] was from Cayman Chemical. *N*-[5-(Dimethylamino)naphthalene-1-sulfonyl]-1,2-dihexadecanoyl-*sn*-glycero-3-phosphoethanolamine (dansyl-PE or dPE) was from Invitrogen, and cholesterol (CH) was from Sigma.

Inositol 1,2,3,4,5,6-hexakisphosphate (IP_6) was from Sigma, and inositol 1,3,4,5-tetrakis(phosphate) (IP_4) was from CellSignals, Inc. CoA trilithium salt and reduced glutathione were from Sigma; dithiothreitol (DTT) was from Research Products International. 2-Mercaptoethanol (BME) was from Fluka; glutathione Sepharose 4B Media was from GE Healthcare Life. Alexa Fluor 555 (AF555) C2-maleimide and perfusion chamber gaskets for single-molecule studies were from Invitrogen.

Protein Preparation of Purified PH Domains. For single-molecule measurements of particle brightness and diffusion, human WT and T513E PDK1 PH domains were engineered to introduce the 11-residue Sfp labeling tag[26] at the N-terminus and were expressed in *Escherichia coli* strain Rosetta 2(DE3) as GST fusion proteins as described for other PH domain constructs.[23,27] Following isolation on a glutathione affinity column, the PH domains were enzymatically labeled with Alexa Fluor 555 (AF555) and the GST tag was removed proteolytically (using thrombin) to generate the isolated, labeled PH domain as previously described.[23,27]

For ensemble measurements of target membrane affinity and association kinetics, human WT and T513E PDK1 PH domains were expressed in Sf9 insect cells and purified as previously described.[2] Mass spectrometry analysis revealed that neither PH domain was modified by phosphorylation or by any other post-translational modification.

Membrane Preparation. For single-molecule TIRF microscopy measurements, supported lipid bilayers were created containing target lipid PIP_3 in the 74/24/2 PC/PS/PIP_3 simple lipid mixture. These supported bilayers were deposited on the surface of a glass slide within a perfusion chamber, as previously described.[22,23]

For ensemble measurements of target membrane affinity and association kinetics, plasma membrane-like membranes were generated as 27.5/10.5/21/4.5/4.5/25/5/2 PE/PC/PS/PI/SM/CH/dPE/PIP_3 sonicated unilamellar vesicles (SUVs) to mimic the plasma membrane inner leaflet.[24,25,28] All lipids were dissolved in chloroform except PIP_3, which was dissolved in a chloroform/methanol/water mixture (1/2/0.8). Subsequently, the plasma membrane-like lipid mixture was created at the indicated mole ratios and dried under vacuum until all the solvent was removed and then hydrated by being vortexed with physiological buffer [25 mM *N*-(2-hydroxyethyl)piperazine-*N*′-2-ethanesulfonic acid (HEPES) (pH 7.4 with KOH), 140 mM KCl, 15 mM NaCl, and 0.5 mM $MgCl_2$]. Finally, SUVs were prepared using a Misonix XL2020 probe sonicator as previously described, yielding a total lipid concentration of 3 mM.[24,25]

TIRFM Single-Molecule Measurements. Single-molecule TIRFM experiments were conducted on a home-built objective-based TIRFM instrument, as described previously,[23,27] but with improvements to include a larger field of view and two laser lines. Glass-supported lipid bilayers were imaged before and after the addition of physiological buffer (above, containing also 5 mM reduced glutathione) and protein to account for nonprotein contaminants, which were typically few in number. After addition of protein, the perfusion imaging assembly was allowed to equilibrate for 5 min to an ambient room temperature of 22.5 ± 0.6 °C. A high-power laser pulse was used to photobleach immobile protein aggregates, after which the fluorescence was allowed to recover for 60 s before data were acquired. Data streams were recorded at a rate of 20 frames/s at a spatial resolution of 4.4 pixels/μm using NIS-Elements BR (Nikon). As in our previous studies, ImageJ and the associated Particle Tracker plugin were used to track the trajectories of fluorescent bilayer-resident particles.[23,27] Resulting data were imported into Mathematica (Wolfram Research) GraphPad Prism 5 (GraphPad Software, Inc.) and OriginPro (OriginLab) for subsequent analysis.[23,27] Stringent filters were applied to exclude bright protein aggregates, dim nonprotein contaminants, immobile particles, rapidly dissociating or nonspecifically bound particles, and overlapping tracks.[22,23,27]

Single-Molecule Fluorescence Studies of Particle Brightness on Supported Lipid Bilayers. After single particles had been filtered to exclude excessively bright, dim, fast, and slow data, the Particle Tracker-generated intensities were used to generate a frequency distribution of brightness values. The evanescent illumination intensity across the TIRF field was analyzed and found to be homogeneous, indicating there was no illumination bias in the monitored region. For a given single-molecule trajectory, Particle Tracker generated an integrated intensity or brightness for each diffusion step. For hundreds of trajectories, these brightness values were binned by relative brightness and used to generate a frequency distribution of single-particle brightness.

Photobleaching or dissociation events were identified as trajectories with a two-step or one-step intensity dimming. Data were manually fit to a step function by averaging the stable intensity values pre- and postdimming, yielding average intensity values representing states where one and two functional fluorophores are detected, respectively.

Single-Molecule Fluorescence Studies of Two-Dimensional (2D) Diffusion on Supported Lipid Bilayers. To resolve the mixed population of PDK1 PH monomers and dimers on the basis of their different lateral diffusion speeds, a strategy was employed that was previously used to analyze a population of mixed monomers and dimers on the supported bilayer surface.[23] Briefly, a combination of Mathematica and GraphPad Prism algorithms were used to determine a diffusion constant for each individual trajectory, and subsequently to generate diffusion coefficient distributions. For each individual trajectory that passed our filtering criteria, a mean displacement between adjacent frames ($\langle r^2 \rangle_{traj}$) was calculated and used to determine the apparent diffusion coefficient (D_1) for a single track:

$$D_1 = \langle r^2 \rangle / (4\Delta t) \quad (1)$$

After an empirical correction had been applied,[29] the resulting single-track diffusion coefficients were binned to generate a frequency distribution that was fit by one or two Lorentzian functions as appropriate.

Ensemble Fluorescence Studies of Equilibrium Binding. Equilibrium binding measurements were conducted on a Photon Technology International QM-2000-6SE steady state fluorescence spectrometer at 25 °C in physiological buffer (see above) with 10 mM DTT as previously described.[24,25] For intrinsic Trp emission experiments, excitation and emission wavelengths were 284 and 335 nm, respectively, and excitation and emission slit widths were 1 and 8 nm, respectively. For protein-to-membrane FRET experiments, excitation and

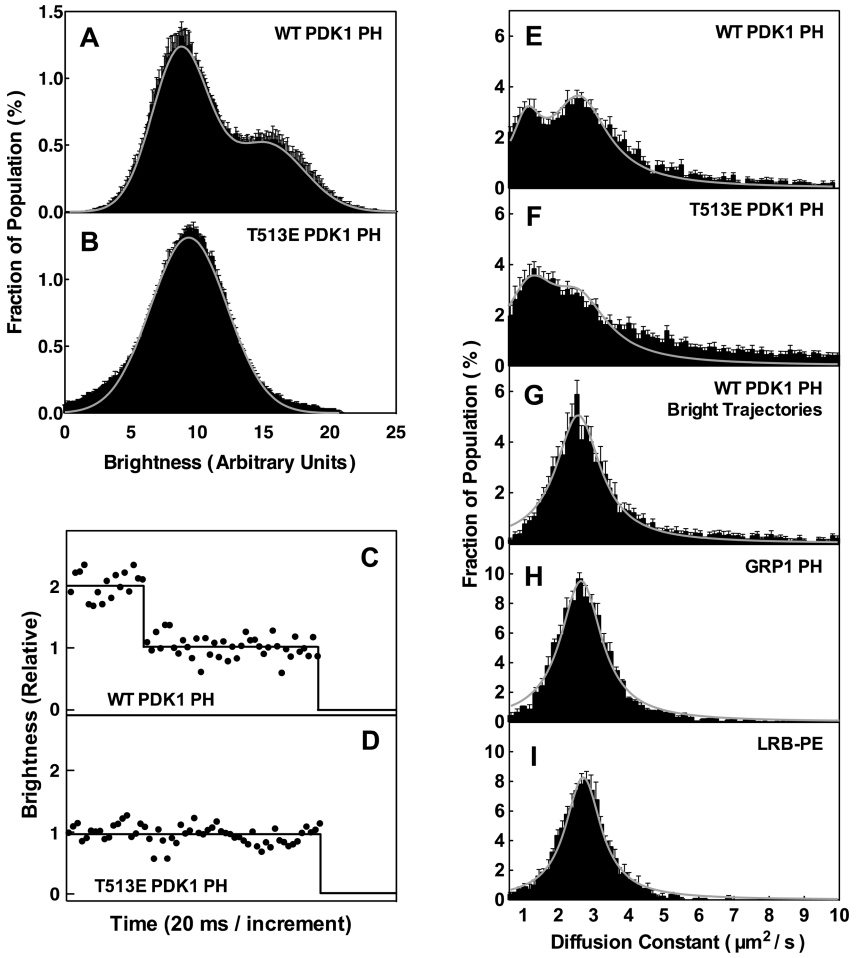

Figure 2. Single-molecule TIRFM analysis of Alexa Fluor 555-labeled PDK1 PH domains bound to PIP_3-containing supported lipid bilayers. (A and B) Single-particle brightness distributions for WT and T513E PH domains. Each single particle was identified as a 2D diffusion track, and the brightness of the particle was integrated in each 20 ms frame and binned with the single-frame brightnesses of hundreds of other single particles from two different movies to generate the indicated brightness distribution. The breadth of each distribution arises from the diffusional motion that spreads out a given particle and introduces uncertainty into its integration. Each fitted curve (gray line) was determined by nonlinear least-squares best fitting of Guassian distributions. (C and D) Representative brightness time courses of single particles of WT and T513E PH domains bound to PIP_3 on supported lipid bilayers, illustrating the stepwise loss of individual fluors caused by bleaching or dissociation. (E–I) Single-particle, 2D diffusion analysis of fluor-labeled PH domains and lipids on supported lipid bilayers. Each distribution shows the relative probabilities of binned, single-particle 2D diffusion constants each determined from one diffusion track as previously described.[30] The breadth of each distribution arises from the uncertainty in the diffusion constant estimated from a limited number of steps. Fitted curves (gray lines) were determined by nonlinear least-squares best fitting of Lorentzian distributions. For panels A–I, all SM TIRFM measurements were taken at 22 °C in physiological buffer on 74/24/2 PC/PS/PIP_3 supported bilayers (Materials and Methods).

emission wavelengths were 284 and 522 nm, respectively, and excitation and emission slit widths were 1 and 8 nm, respectively.

The previously described competitive displacement assay was used to quantitate the high-affinity binding of each PH domain to plasma membrane-like bilayers at 25 °C in physiological buffer (see above).[24,25,28] This approach begins with measurement of the affinity of the free PH domain for the competitive inhibitor IP_6 in solution, which is quantitated by monitoring the increase in PH domain intrinsic Trp fluorescence upon IP_6 binding. The resulting IP_6 binding curve yields the equilibrium dissociation constant for inhibitor binding, K_{DI}, as previously described.[24,25,28] Subsequently, the competitive inhibitor is titrated into the PH domain–membrane complex and protein-to-membrane FRET monitored to quantitate the competitive displacement of the PH domain from its PIP_3 target lipid. The resulting competitive displacement curve yields equilibrium inhibition constant K_I as previously described.[24,25,28] Finally, the equilibrium dissociation constant for the target PIP_3 lipid on plasma membrane-like bilayers, K_{DPIP3}, is calculated:

$$K_{DPIP3} = [PIP_3]_{free}/[(K_I/K_{DI}) - 1] \quad (2)$$

Equation 2 shows that it is useful to use a total PIP_3 concentration (3 μM accessible) in the competitive displacement titration that is large compared to the total PH domain concentration (0.5 μM), so that the free PIP_3 concentration can be approximated as the total PIP_3 concentration. The described approach using the inexpensive competitive inhibitor IP_6 successfully determined K_{DPIP3} for the lower-affinity T513E PH domain but failed to yield a quantitative K_{DPIP3} for the higher-affinity WT PH domain. Thus, it was necessary to conduct additional competitive displacement studies with the higher-affinity, but costly, competitive inhibitor IP_4. The approach described above for IP_6 was therefore modified as follows to preclude the need for expensive IP_4 titrations of the free PH domains to determine the IP_4 K_{DI}. For each PH

dx.doi.org/10.1021/bi400488f | Biochemistry 2013, 52, 4820–4829

domain, a standard competitive displacement titration with IP_4 was conducted to measure the IP_4 K_I for the domain bound to target membranes. For the T513E PH domain, the known K_{DPIP3} and the measured IP_4 K_I were used to calculate the IP_4 K_{DI} using eq 2. Because IP_6 and IP_4 bind to the same headgroup binding cleft, and because the mutation is far from this cleft, it is reasonable to assume that the IP_6 K_{DI}/IP_4 K_{DI} ratio is the same for the T513E and WT PH domains, thereby allowing calculation of IP_4 K_{DI} for the WT domain from the measured values of IP_6 K_{DI} for both domains and the calculated value of IP_4 K_{DI} for the mutant. Finally, eq 2 was successfully used to calculate K_{DPIP3} for the WT PH domain from the calculated IP_4 K_{DI} and the measured IP_4 K_I. Nonlinear least-squares best fits were used to determine the best fit K_{DI} and K_I parameters and their error ranges as previously described.[24,25,28]

Ensemble Fluorescence Studies of Association Kinetics. Ensemble kinetic studies were conducted on an Applied Photophysics SX.20 stopped-flow fluorescence instrument to monitor changes in protein-to-membrane FRET during the time course of binding of the PH domain to plasma membrane-like membranes in physiological buffer with 10 mM DTT at 25 °C as previously described.[24,25,28] The PH domain (1 μM) was rapidly mixed by a stopped-flow method with plasma membrane-like SUVs (total lipid concentration of 600 μM) containing excess PIP_3 target lipid (6 μM accessible), leading to final concentrations of 0.5 μM PH domain and 3 μM accessible PIP_3. Under these conditions, the forward binding reaction is virtually irreversible because of the high affinity of the PH domain for the PIP_3 lipid, and best fit analysis of the binding time course with a single-exponential component for binding to homogeneous sites yielded the apparent on rate constant [$k_{on(app)}$], calculated as previously described.[24,25,28]

RESULTS

Determining the Oligomeric State of the Membrane-Bound PH Domain by Single-Molecule Brightness Analysis. Models 1 and 2 predict that the WT and T513E PDK1 PH domains bound to PIP_3 on a target membrane will be homodimeric and monomeric, respectively, while model 3 predicts that both domains will be monomeric (Figure 1). To resolve these predictions, single-molecule total-internal-reflection-microscopy (SM TIRFM) analysis was conducted to investigate the oligomeric state of the WT and mutant PH domains while bound to the target PIP_3 lipid on a supported bilayer.[22,23,27] The method tracks individual fluorescent proteins, which can be monomers or oligomers, diffusing in two dimensions on the membrane surface. Engineered WT and T513E PH domains possessing 11-residue labeling tags at their N-termini were enzymatically labeled with the relatively photostable Alexa Fluor 555 and purified by exhaustive buffer exchange. This protocol allows specific labeling at a non-perturbing site even in proteins possessing intrinsic Cys residues (such as Cys 536 in the PDK1 PH domain) and yields up to ~50% labeling efficiency under the mild labeling conditions used herein that are designed to preserve full biological activity.[23,27] A simple lipid mixture (74/24/2 PC/PS/PIP_3) was used to generate supported bilayers, which previous SM TIRFM studies of PIP_3-bound PH domains have shown yields rapid, homogeneous 2D diffusion.[22,23] SM TIRFM analysis of WT and T513E PH domains showed that PIP_3 was required for stable bilayer association, confirming that labeling and purification yielded well-folded PH domains possessing native PIP_3 specificity. Notably, to generate the same density of membrane-associated single particles, an ~10-fold [9.7 ± 1.9 (standard error); n = 3] higher concentration of the T513E PH domain was needed relative to the concentration of the WT PH domain. The binding reactions are far from saturation and in the linear region ([PH-PIP_3] ~ K_B[PIP_3][PH]); thus, the mutant possesses an ~10-fold lower affinity for the target PIP_3 bilayer.

Brightness analysis can directly detect membrane-bound oligomers containing two fluors, which are twice as bright as single fluors and bleach in two steps rather than one. For both the WT and the mutant PH domain, brightness distributions were measured for large populations (>5000) of single fluorescent particles diffusing on the target supported bilayer. Figure 2A shows that a representative WT distribution exhibits two subpopulations with average brightnesses differing by approximately 2-fold (arbitrary brightness units of 9 ± 2 and 15 ± 3, respectively). The relative sizes of these bright and dim subpopulations are consistent with a binomial distribution of WT dimers in which 53 and 47% of the membrane-associated subunits are labeled and unlabeled with the fluorescent probe, respectively (as expected for the partial labeling generated by the enzymatic protocol). Such a distribution would generate a mixed population of WT dimers in which 28% possess two fluors, 50% possess one fluor, and 22% possess no fluor, thereby yielding the observed ratio of the bright to dim subpopulations (28/50 = 0.56; the unlabeled dimers are invisible). Moreover, the fluorescence of bright WT particles can be observed to disappear in two steps as illustrated in Figure 2C, where each step represents the loss of one fluorophore by bleaching or dimer dissociation, confirming these bright particles possess two fluors. Thus, brightness analysis of the WT PH domain indicates the observed membrane-bound particles are predominantly dimers, although the data cannot rule out a small subpopulation of monomeric PH domains.

In contrast to the WT PH domain, the T513E PH domain exhibits brightness distributions that are homogeneously dim (Figure 2B), exhibiting the same brightness as the dim WT subpopulation (9 ± 3 and 9 ± 2, respectively). Moreover, when mobile T513E PH domains disappear because of bleaching or membrane dissociation, no multistep brightness decreases are detected (Figure 2D). Thus, the mutant protein is predominantly monomeric on the membrane surface, although the data cannot exclude a small population of dimeric PH domains.

Overall, the brightness analysis rules out model 3 in which both membrane-bound WT and T513E PH domains are predicted to be monomeric. Instead, the brightness data are consistent with models 1 and 2, which both predict that the WT PH domain is dimeric and the mutant PH domain is monomeric. However, the brightness analysis cannot resolve models 1 and 2, which are distinguished by their contrasting predictions that the WT domain binds one and two molecules of the PIP_3 target lipid, respectively.

Analyzing Lipid and Bilayer Contacts by Single-Molecule Diffusion Analysis. Previous studies of peripheral proteins on supported bilayers have shown that the 2D diffusion measurements can detect lipid binding and bilayer penetration, because protein−lipid and protein−bilayer interactions generate friction with the bilayer and decrease the lateral diffusion constant.[27,30] At the rapid 2D diffusion limit, the GRP1 PH domain has been shown to bind a single PIP_3 lipid with minimal bilayer penetration, yielding the same diffusion constant as a free lipid in the bilayer, because the

dx.doi.org/10.1021/bi400488f | Biochemistry 2013, 52, 4820−4829

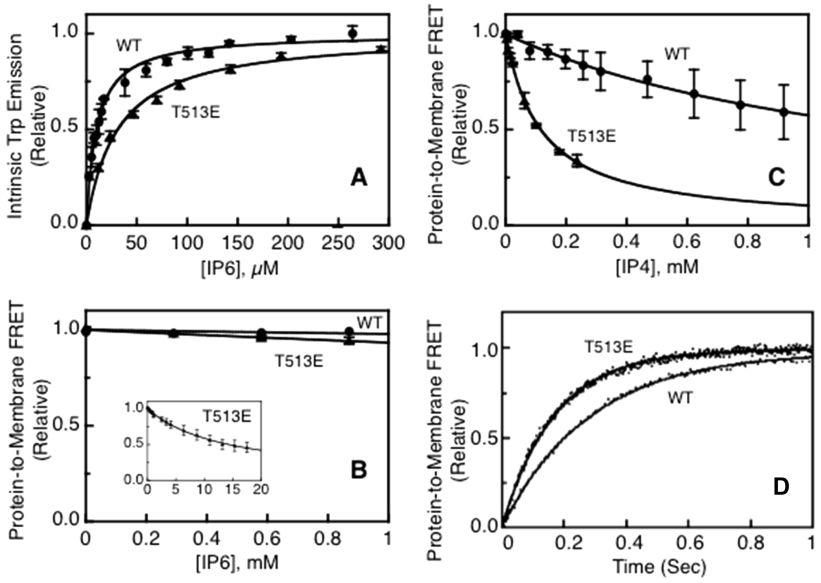

Figure 3. Measurement of equilibrium affinities and on rates for binding of PDK1 PH domains to PIP_3 on plasma membrane-like target membranes. (A) IP_6 affinity titrations for free WT and T513E PDK1 PH domains in solution, where binding of IP_6 to the PH domain is quantitated by the resulting intrinsic Trp fluorescence increase as previously described.[24,25,28] (B) Competitive displacement titrations using protein-to-membrane FRET to monitor dissociation of the PH domain from PIP_3 target membranes while the competitive inhibitor IP_6 is titrated into the sample as previously described.[24,25,28] (C) Same as panel B using IP_4 as the competitive inhibitor. (D) Measurement of association kinetics for binding of PDK1 PH domains to PIP_3 on plasma membrane-like target membranes. Shown are the time courses of binding of WT and T513E PDK1 PH domains to PIP_3 following stopped-flow rapid mixing of the PH domain with target membranes, using protein-to-membrane FRET to quantitate membrane association as previously described.[24,25,28] All experiments were conducted at 25 °C in physiological buffer using plasma membrane-like bilayers (Materials and Methods). Fitted curves (—) were determined by nonlinear least-squares best fit analysis for homogeneous populations of binding sites.

friction of the protein−lipid complex is dominated by the contacts of the bound lipid with the viscous bilayer.[22] The binding of additional lipids or penetration of the protein into the bilayer can slow lateral diffusion up to 10-fold relative to that of the GRP1 PH domain.[30]

To investigate the diffusion of the WT PH domain on supported bilayers, the diffusion track of each fluorescent particle was quantified and used to calculate an average diffusion constant D_i for that particle. Hundreds of single-particle diffusion constants were determined and used to construct the WT distribution illustrated in Figure 2E. The WT domain exhibits two distinct subpopulations of diffusing species: a major, fast subpopulation ($D \sim 2.6\ \mu m^2/s$) and a minor, slow subpopulation ($D \sim 1.1\ \mu m^2/s$). To determine which peak is representative of the dimeric WT PH domain, 2-fold brighter dimeric particles in the brightness distribution of Figure 2A were identified and their diffusion tracks are summarized in a distribution of single-particle diffusion constants, as illustrated in Figure 2G. It is evident that the bright dimer diffusion exhibits only the fast component of the WT distribution (compare panels E and G of Figure 2), and the homogeneity of the resulting distribution allows an accurate average dimer diffusion constant to be determined ($D = 2.6 \pm 0.9$). Strikingly, a very similar distribution of single-particle diffusion coefficients is observed for the GRP1 PH domain bound to a single PIP_3 lipid, yielding the same average diffusion constant ($D = 2.6 \pm 0.9$) as shown in Figure 2H. Moreover, this identical diffusion constant observed for WT PDK1 and GRP1 PH domains matches that of a single, free lipid molecule diffusing in the bilayer (compare panels G−I of Figure 2). Together, these findings indicate that most (>80% by integration of the two components in Figure 2E) of the dimeric WT PDK1 PH domains diffusing on the membrane surface are tightly bound to a single PIP_3 lipid with little or no penetration of the protein into the bilayer, as previously observed for the GRP1 PH domain.[22,31]

The T513E PH domain also exhibits a bimodal distribution with slow and fast components possessing diffusion constants similar to those observed for the WT domain, but unlike the WT domain, the slow component of the mutant is more prevalent (>80% by integration of the two components) as illustrated in Figure 2F. The fact that slow and fast components are observed for both WT and T513E in different proportions provides strong evidence that the T513E mutation shifts an equilibrium between a slow monomeric state and a fast dimeric state. Brightness filtering of the WT domain to select only dimers removes the slow component, consistent with the interpretation that the slow diffusion state is accessible to only the monomeric PH domain (Figure 2G).

The diffusion analysis supports model 1 and strongly disfavors model 2. GRP1 PH domain constructs that bind two PIP_3 lipids exhibit up to 2-fold slower diffusion than a single lipid, or a native GRP1 PH domain bound to a single lipid.[23,27] Although the dimeric WT PDK1 PH domain possesses two PIP_3 binding sites, it diffuses at the same rapid rate as a single lipid, and as the native GRP1 PH domain bound to a single lipid (compare panels G−I of Figure 2), indicating this WT dimer binds one PIP_3 lipid, not two. Similarly, the monomeric T513E mutant exhibits a small population of this fast component, consistent with the occupancy of its single PIP_3 binding site by one PIP_3 lipid. The dominant slowly diffusing population of the monomeric T513E mutant (Figure 2F) also possesses just one PIP_3 binding site, and its slower diffusion suggests this state allows additional penetration of the

dx.doi.org/10.1021/bi400488f | Biochemistry 2013, 52, 4820−4829

Table 1. Equilibrium and Kinetic Parameters for Binding of PH Domains to Plasma Membrane-like Bilayers Containing PIP_3

	equilibrium[a]				kinetics[a]	
	$K_D(IP_6)$ (μM)	$K_D(IP_4)$ (μM)	$K_I(IP_4)$ (mM)	$K_D(PIP_n)$ (nM)	$k_{on(app)}$ (μM^{-1} s^{-1})	$k_{off(calc)}$ (ms^{-1})
PDK1 WT PH	9 ± 3	0.11 ± 0.02	1.3 ± 0.5	0.2 ± 0.1	1.6 ± 0.1	0.3 ± 0.2
PDK1 T513E PH	30 ± 11	0.32 ± 0.07	0.12 ± 0.01	7 ± 2	2.5 ± 0.1	18 ± 5

[a]All parameters determined as described in Materials and Methods.

PH domain into the bilayer that increases friction and slows lateral movement. The minor slow population is not observed for the isolated WT dimers (Figure 2G), suggesting that the slow state can exist for only the monomeric PH domain. The simplest explanation is that the structure of the dimeric PH domain prevents insertion of the protein into the bilayer that is the hallmark of the slowly diffusing state.

Target Membrane Affinities of WT and T513E PH Domains. The single-molecule studies described above suggested that WT and T513E PH domains possess significantly different bilayer affinities, because an ~10-fold higher concentration of mutant PH domain is needed to generate the same density of membrane-bound protein. To quantify this difference, further equilibrium bulk membrane binding assays were conducted using a near physiological mixture of lipids matching the composition of the plasma membrane inner leaflet to maximize the relevance to cellular conditions.[24,25,28] Purified PH domains were mixed with sonicated, unilamellar, plasma membrane-like bilayers (27.5/10.5/21/4.5/4.5/25/5/2 PE/PC/PS/PI/SM/CH/dPE/PIP_3). The resulting population of proteins bound to PIP_3 on the target membrane surface was monitored by protein-to-membrane FRET using the four intrinsic Trp residues of the PH domain as donors and a small mole percent (5%) of membrane-incorporated dansylated phosphatidylethanolamine (dPE) as the acceptor. Subsequently, a competitive inhibitor of known affinity for the free PH domain was titrated into the system, and the resulting displacement of the PH domain from the target membrane was measured as illustrated in Figure 3. This FRET competitive displacement assay has previously been shown to be especially useful in quantifying target membrane affinities in the nanomolar to subnanomolar range where direct binding measurements are difficult.[24,25,28]

Initial titrations utilized IP_6 as a competitive inhibitor, because this highly phosphorylated inositol typically binds to PIP_3-specific PH domains with an affinity in the range of 1−300 μM.[24,25,28] Such affinity is usually sufficient to displace PH domains from PIP_3 on target membranes, as observed for AKT1 and GRP1 PH domains.[24,25,28] The IP_6 binding curves in Figure 3A were used to measure the affinities of the WT and T513E PDK1 PH domains for this inhibitor, employing the intrinsic Trp fluorescence change that occurs when IP_6 binds to the free PH domain in solution.[24,25,28] The titrations reveal that WT and T513E PDK1 PH domains possess similar IP_6 affinities in the standard range (K_D values of 9 ± 3 and 30 ± 10 μM, respectively). However, IP_6 is a poor competitive inhibitor for binding of the WT PDK1 PH domain to PIP_3 on target membranes, as illustrated in Figure 3B, where 1 mM IP_6 displaces <5% of the membrane-bound protein. These findings indicate that the affinity of the WT PDK1 PH domain for PIP_3 target membranes is considerably higher than that previously observed for AKT1 and GRP1 PH domains, and that a competitive inhibitor with an affinity higher than that of IP_6 is needed. The chosen inhibitor was inositol 1,3,4,5-tetraphosphate (IP_4), which is the isolated headgroup of the PIP_3 target lipid and thus exhibits maximal affinity for the highly specific ligand binding pocket of the PDK1 PH domain.

The IP_4 titrations of WT and T513E PDK1 PH domains were successful, yielding the target membrane affinities for both proteins. The WT domain exhibits an 80-fold higher affinity for IP_4 than for IP_6 (Table 1), facilitating the quantitative IP_4 titrations as illustrated in Figure 3C. The resulting target membrane affinities of WT (K_D = 0.2 ± 0.1 μM) and T513E (K_D = 7 ± 2 μM) PDK1 PH domains are summarized in Table 1. The 35-fold greater PIP_3 membrane affinity observed for the dimeric WT protein relative to the monomeric mutant is slightly larger than the ~10-fold difference observed in the single-molecule studies (see above), suggesting that the plasma membrane-like lipid composition enhances the affinity difference. However, even the 35-fold affinity enhancement represents an only 1.2-fold stabilization of the total binding free energy, consistent with a model in which the dimeric PH domain possesses enhanced binding affinity for a single PIP_3 lipid and does not bind a second PIP_3 lipid. This finding strongly supports model 1 and disfavors model 2, because the latter model proposes the dimeric WT domain binds two PIP_3 lipids and thus should exhibit an ~2-fold stabilization of binding free energy relative to monomeric T513E.

Ensemble Kinetic Measurements Comparing WT and T513E PH Domains. To further investigate the mechanism of target membrane binding, ensemble kinetic experiments were designed to measure the on and off rate constants (k_{on} and k_{off}, respectively) for binding of the PH domain to PIP_3 target membranes. Standard ensemble fluorescence methods employing stopped-flow fluorescence and protein-to-membrane FRET were used to investigate the time courses of membrane binding and dissociation, respectively.[24,25,28]

Association time courses were triggered by stopped-flow rapid mixing of plasma membrane-like target membranes with the free PH domain, followed by protein-to-membrane FRET quantitation of membrane binding as illustrated in Figure 3D and Table 1. The resulting time courses reveal that WT and T513E domains possess k_{on} values within 2-fold of each other (1.6 ± 0.1 and 2.5 ± 0.1 μM^{-1} s^{-1}, respectively). This observation supports the conclusion that both domains bind a single PIP_3 target lipid and thus exhibit similar on rates.

Attempts to directly measure dissociation kinetics were unsuccessful because of the high PIP_3 affinity of the domains and the unavailability of a competitive inhibitor that binds the PH domain tightly enough to make PIP_3 dissociation irreversible. However, the dissociation rate constant can be estimated from the measured K_D and k_{on} parameters as summarized in Table 1. The calculations imply that the PIP_3 affinity difference between WT and T513E domains arises primarily from the slower dissociation of WT from the PIP_3 target lipid on the plasma membrane-like bilayer.

Overall, the preponderance of kinetic evidence is consistent with a picture in which both the WT PDK1 PH domain dimer and the T513E mutant monomer bind to a single PIP_3 lipid on the target membrane surface. The dissociation of the dimer by

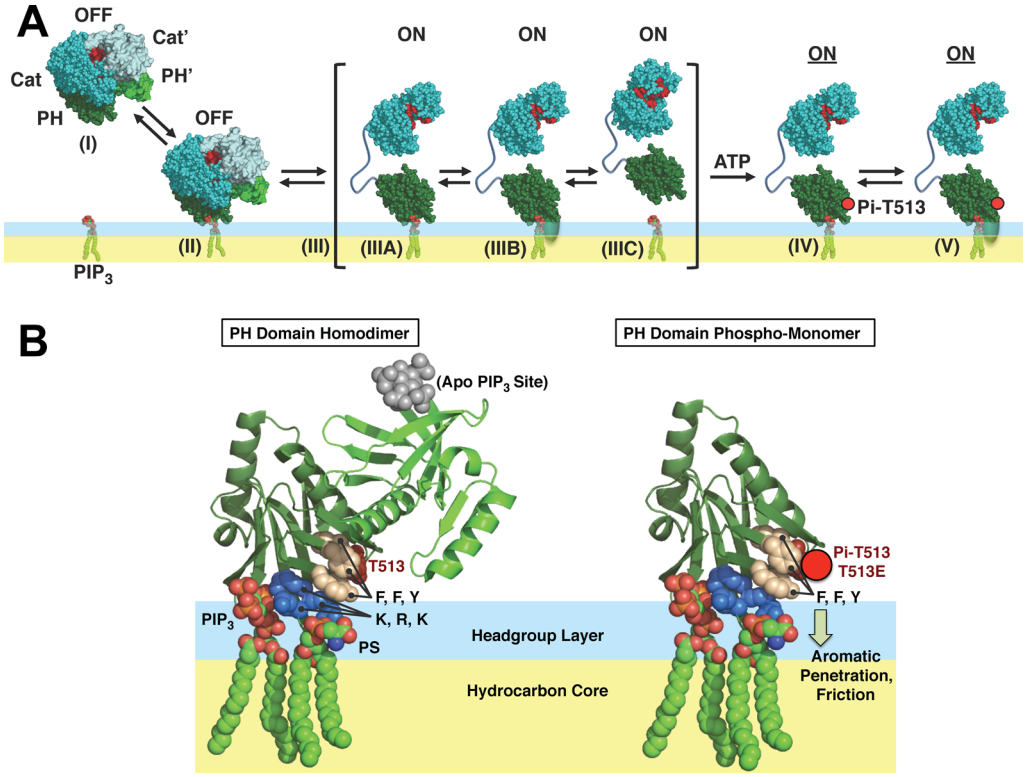

Figure 4. Model for the activation mechanism of PDK1, controlled by the phospho-activated dimer-to-monomer conversion of the PH domain. (A) Overview of the proposed mechanism for full-length PDK1. The inactive dimer (I) is recruited to the membrane by a PIP_3 signal, where it binds to a single PIP_3 lipid (II). During a transient dimer dissociation event (III), a given monomer can exist in a shallow membrane docking state (preferred, IIIA) or a more deeply penetrating state (IIIB), or, occasionally, a dissociated state (IIIC) that might rebind to another PIP_3 before diffusing away from the membrane. Following this transient dimer dissociation, the two monomers either reassociate to form the active dimer or become autophosphorylated at PH domain position T513 that traps the monomeric state (IV) by destabilizing the dimer interface and allowing the aromatics to insert into the bilayer (symbolized by the schematic oval), thereby slowing diffusion (V). (B) Schematic molecular views of the membrane-associated PH domain dimer and monomer. Shown are basic side chains (medium blue) involved in binding one PIP_3 lipid and one adjacent PS lipid (indicated). Highlighted also are aromatic side chains (tan; F514, F515, and Y524) in van der Waals contact with the adjacent T513 residue. The negative charge of the phospho-T513 side chain is proposed to destabilize local folding, thereby weakening the dimer interface and PIP_3 affinity while facilitating insertion of the aromatic side chains into the bilayer. Such local unfolding cannot occur in the WT dimer because dimerization stabilizes the folded state and the other subunit sterically prevents the insertion of aromatics into the bilayer. PH domain crystal structure from PDB entry 1W1H.[21]

the phospho-mimetic T513E mutation lowers the PIP_3 affinity and decreases the bound state lifetime; both these effects could play important roles in the signaling biology of PDK1.

DISCUSSION

The findings are consistent with a novel PDK1 activation model presented in Figure 4A. The cytoplasmic, inactive state of PDK1 is hypothesized to be a homodimer stabilized by interactions between the two PH domains, as previously proposed. The structure of the PH domain dimer is likely similar to that of the nearly *C*2 symmetric dimer seen in the unit cell of the PH domain crystal structure (PDB entry 1W1H[21]) and to that of the closely related *C*2 symmetric dimer modeled using this crystallographic dimer as a starting point.[2] For both the crystallographic and modeled PH domain dimers, the structure allows binding of only one subunit to a PIP_3 headgroup, because binding to the first PIP_3 orients the PIP_3 binding pocket of the other subunit away from the bilayer surface (Figure 4B). The docking of the first PH domain subunit to PIP_3 is proposed to generate minor steric clashes between the other subunit and the bilayer that can be largely accommodated by the flexibility of the dimer but lower the dimer stability and occasionally lead to transient dimer dissociation, thereby accounting for the small population of the monomer observed in the diffusion analysis of the WT PH domain (Figure 2E). Dissociation of the dimer is proposed to enable *cis* or *trans* phosphorylation of PH domain residue T513 by the kinase domain of the same monomer or of an adjacent PDK1 monomer, respectively. The resulting negative charge at the T513 position is hypothesized to destabilize the local PH domain structure because of unfavorable interactions with the adjacent F514, F515, and Y524 aromatic rings, which contact the T513 side chain in the PH domain crystal structure. The resulting local destabilization, in turn, is proposed to disrupt the dimer interface, decrease PIP_3 affinity, and allow multiple aromatic side chains, including F513 and Y524, to penetrate the bilayer. In the dimer, these aromatic side chains are sterically prevented from inserting into the bilayer (Figure 4B), but in the monomer, their insertion increases friction against the viscous bilayer, thereby slowing lateral diffusion (Figure 2F).

Overall, the model accounts for the observed ability of the T513E mutation, which mimics phosphorylation of T513, to convert the dimer (Figure 2A) completely to the monomer (Figure 2B). In the monomeric state, the steric occlusion of the kinase domain active site proposed for the dimer[2] is removed, thus yielding the active enzyme. Moreover, in the monomeric

dx.doi.org/10.1021/bi400488f | *Biochemistry* 2013, 52, 4820−4829

state, the protein interaction surfaces of the PH and kinase domains are available for docking to substrate proteins such as AKT/PKB. To ensure effective control of activation by T513 phosphorylation, it is important that the population of slowly diffusing monomer observed for the WT PH domain be a minor component as observed (Figure 2E); in full-length PDK1, this monomeric unphosphorylated component would be even less prevalent, assuming that interactions between kinase domains further stabilize the dimer as proposed.[2] The model also accounts for the lower affinity of the T513E mutant for PIP_3-containing target membranes, because it is reasonable to propose that the local structural disruption triggered by the phospho-mimetic mutation would significantly perturb the PIP_3 binding pocket that largely defines the membrane affinity. Thus, even though the mutant buries more hydrophobic surface area in the bilayer, the perturbation of the PIP_3 binding pocket yields a net loss of membrane affinity. Finally, the model accounts for the observed fast diffusion of the dimeric protein (Figure 2G), as well as the generally slower diffusion of the monomer (Figure 2F).

It is not surprising that the PDK1 PH domain dimer diffuses at the same rate as a single free lipid molecule in the bilayer (Figure 2I), like the monomeric GRP1 PH domain (Figure 2H). Both the PDK1 PH dimer and the GRP1 PH monomer bind a single PIP_3 lipid that penetrates deeply into the membrane and dominates the friction between the protein−lipid complex and the highly viscous bilayer. Both proteins also interact with PS,[22,28,32] but the contribution of this additional interaction to friction is negligible, either because PS binding is transient or because the bound PIP_3 and PS lipids are nearly adjacent in the structure, ensuring they are far from the free draining limit such that their movements are highly coupled and resemble the movements of a single lipid.[27,30,33] The GRP1 PH domain binds the large PIP_3 headgroup that projects out from the membrane surface, requiring little penetration of the protein into the bilayer for effective headgroup contacts,[31] and the similar diffusion rate observed for the WT PDK1 PH domain suggests a similar, shallow membrane docking with little protein penetration. The 2-fold greater protein mass of the PDK1 PH domain dimer does not significantly slow diffusion because the protein exposed to the aqueous phase makes a negligible contribution to friction; as previously observed, friction is instead dominated by contacts with the bilayer, which is ∼100-fold more viscous than water and completely defines the 2D diffusion constant.[22,27,30] For example, linking a water-exposed PH domain with a nonfunctional PIP_3 binding site to a functional PH domain bound to PIP_3-containing target membrane has no effect on the membrane diffusion of the latter domain,[27] which is analogous to the PDK1 PH domain dimer that diffuses like a single PH domain. By contrast, as noted for the proposed diffusional slowing triggered by the phospho-mimetic T513E mutation, the isolated C2 domain of PKCα1 inserts more deeply into the bilayer upon binding PIP_2,[34,35] yielding slower 2D diffusion.[30]

The unusually high PIP_3 affinity of the WT dimer, >1 order of magnitude higher than that observed for monomeric AKT1 and GRP1 PH domains,[24,25] could play a physiologically important role in two ways. This high target lipid affinity could recruit PDK1 to the plasma membrane at low PIP_3 levels in the membrane, perhaps at the beginning of a PIP_3 signal. Alternatively, the high PIP_3 affinity could be offset by the steric contacts of the dimer with the bilayer, which could lower the PIP_3 affinity to levels similar to that observed for other monomeric, PIP_3-specific PH domains. The significantly lower PIP_3 affinity and bound state lifetime of the T513E PDK1 PH domain are predicted to facilitate the release of activated PDK1 to the cytoplasm, where it phosphorylates important cytoplasmic targets, including classical protein kinase C isoforms.

Interestingly, the WT and T513E distributions of lateral diffusion constants possess long tails with high diffusion rates that are faster than that of a free lipid in the bilayer (Figure 2E−G), suggesting that that PDK1 PH domain may possess a search mechanism that accelerates diffusion across the membrane surface. This search mechanism could involve the known binding of the PDK1 PH domain to the PS headgroup,[32] which could allow "hopping" of the PH domain across the membrane surface. The close spacing of PS lipids (∼25 mol % of the total lipid) and the electrostatic steering provided by the adjacent, highly cationic PIP_3 binding site could help minimize macroscopic dissociation from the bilayer during search sequences involving multiple rapid hops between stable PIP_3 binding events. This putative search mechanism based on transient binding to PS could be even more efficient than the electrostatic search mechanism previously observed for the GRP1 PH domain.[22,28] Such search mechanisms are essential for rapid binding to the rare target lipid PIP_3, which is present at very low densities even during a PIP_3 signaling event.[22,28] Further studies are needed to test the hypothesized search mechanism for the PDK1 PH domain and to test the predictions of the novel activation mechanism of Figure 4 in full-length PDK1.

AUTHOR INFORMATION

Corresponding Author

*E-mail: falke@colorado.edu. Telephone: (303) 492-3503.

Funding

Support provided by National Institutes of Health Grant R01 GM-063235 (to J.J.F.) and by Cancer Research U.K. and the London Research Institute (to B.L.).

Notes

The authors declare no competing financial interest.

ABBREVIATIONS

PH domain, pleckstrin homology domain; PDK1, phosphoinositide-dependent kinase-1; AKT1/PKB, protein kinase B; GRP1, general receptor for phosphoinositide isoform 1; Sfp, phospho-pantethienyl-transferase; AF555, Alexa Fluor 555; SUV, sonicated unilamellar vesicle; TIRFM, total internal reflection fluorescence microscopy.

REFERENCES

(1) Gao, X., and Harris, T. K. (2006) Role of the PH domain in regulating in vitro autophosphorylation events required for reconstitution of PDK1 catalytic activity. *Bioorg. Chem. 34*, 200−223.

(2) Masters, T. A., Calleja, V., Armoogum, D. A., Marsh, R. J., Applebee, C. J., Laguerre, M., Bain, A. J., and Larijani, B. (2010) Regulation of 3-phosphoinositide-dependent protein kinase 1 activity by homodimerization in live cells. *Sci. Signaling 3*, ra78.

(3) Calleja, V., Laguerre, M., and Larijani, B. (2011) Role of the C-terminal regulatory domain in the allosteric inhibition of PKB/Akt. *Adv. Enzyme Regul. 52*, 46−57.

(4) Wu, W. I., Voegtli, W. C., Sturgis, H. L., Dizon, F. P., Vigers, G. P., and Brandhuber, B. J. (2010) Crystal structure of human AKT1 with an allosteric inhibitor reveals a new mode of kinase inhibition. *PLoS One 5*, e12913.

(5) Newton, A. C. (2010) Protein kinase C: Poised to signal. *Am. J. Physiol. 298*, E395−E402.
(6) Bayascas, J. R. (2010) PDK1: The major transducer of PI 3-kinase actions. *Curr. Top. Microbiol. Immunol. 346*, 9−29.
(7) Andrews, S., Stephens, L. R., and Hawkins, P. T. (2007) PI3K class IB pathway in neutrophils. *Sci. STKE 2007*, cm3.
(8) Primo, L., di Blasio, L., Roca, C., Droetto, S., Piva, R., Schaffhausen, B., and Bussolino, F. (2007) Essential role of PDK1 in regulating endothelial cell migration. *J. Cell Biol. 176*, 1035−1047.
(9) Yoshimura, T., Arimura, N., and Kaibuchi, K. (2006) Signaling networks in neuronal polarization. *J. Neurosci. 26*, 10626−10630.
(10) Lopez-Garcia, L. A., Schulze, J. O., Frohner, W., Zhang, H., Suss, E., Weber, N., Navratil, J., Amon, S., Hindie, V., Zeuzem, S., Jorgensen, T. J., Alzari, P. M., Neimanis, S., Engel, M., and Biondi, R. M. (2011) Allosteric regulation of protein kinase PKCζ by the N-terminal C1 domain and small compounds to the PIF-pocket. *Chem. Biol. 18*, 1463−1473.
(11) Wymann, M. P., Zvelebil, M., and Laffargue, M. (2003) Phosphoinositide 3-kinase signalling: Which way to target? *Trends Pharmacol. Sci. 24*, 366−376.
(12) Zhang, H., He, J., Kutateladze, T. G., Sakai, T., Sasaki, T., Markadieu, N., Erneux, C., and Prestwich, G. D. (2010) 5-Stabilized phosphatidylinositol 3,4,5-trisphosphate analogues bind Grp1 PH, inhibit phosphoinositide phosphatases, and block neutrophil migration. *ChemBioChem 11*, 388−395.
(13) Raimondi, C., and Falasca, M. (2011) Targeting PDK1 in cancer. *Curr. Med. Chem. 18*, 2763−2769.
(14) Maurer, M., Su, T., Saal, L. H., Koujak, S., Hopkins, B. D., Barkley, C. R., Wu, J., Nandula, S., Dutta, B., Xie, Y., Chin, Y. R., Kim, D. I., Ferris, J. S., Gruvberger-Saal, S. K., Laakso, M., Wang, X., Memeo, L., Rojtman, A., Matos, T., Yu, J. S., Cordon-Cardo, C., Isola, J., Terry, M. B., Toker, A., Mills, G. B., Zhao, J. J., Murty, V. V., Hibshoosh, H., and Parsons, R. (2009) 3-Phosphoinositide-dependent kinase 1 potentiates upstream lesions on the phosphatidylinositol 3-kinase pathway in breast carcinoma. *Cancer Res. 69*, 6299−6306.
(15) Carpten, J. D., Faber, A. L., Horn, C., Donoho, G. P., Briggs, S. L., Robbins, C. M., Hostetter, G., Boguslawski, S., Moses, T. Y., Savage, S., Uhlik, M., Lin, A., Du, J., Qian, Y. W., Zeckner, D. J., Tucker-Kellogg, G., Touchman, J., Patel, K., Mousses, S., Bittner, M., Schevitz, R., Lai, M. H., Blanchard, K. L., and Thomas, J. E. (2007) A transforming mutation in the pleckstrin homology domain of AKT1 in cancer. *Nature 448*, 439−444.
(16) Peifer, C., and Alessi, D. R. (2008) Small-molecule inhibitors of PDK1. *ChemMedChem 3*, 1810−1838.
(17) Varnai, P., Bondeva, T., Tamas, P., Toth, B., Buday, L., Hunyady, L., and Balla, T. (2005) Selective cellular effects of overexpressed pleckstrin-homology domains that recognize PtdIns-(3,4,5)P3 suggest their interaction with protein binding partners. *J. Cell Sci. 118*, 4879−4888.
(18) Lemmon, M. A. (2008) Membrane recognition by phospholipid-binding domains. *Nat. Rev. Mol. Cell Biol. 9*, 99−111.
(19) Park, W. S., Heo, W. D., Whalen, J. H., O'Rourke, N. A., Bryan, H. M., Meyer, T., and Teruel, M. N. (2008) Comprehensive identification of PIP3-regulated PH domains from *C. elegans* to *H. sapiens* by model prediction and live imaging. *Mol. Cell 30*, 381−392.
(20) Li, Z., Venable, R. M., Rogers, L. A., Murray, D., and Pastor, R. W. (2009) Molecular dynamics simulations of PIP2 and PIP3 in lipid bilayers: Determination of ring orientation, and the effects of surface roughness on a Poisson-Boltzmann description. *Biophys. J. 97*, 155−163.
(21) Komander, D., Fairservice, A., Deak, M., Kular, G. S., Prescott, A. R., Peter Downes, C., Safrany, S. T., Alessi, D. R., and van Aalten, D. M. (2004) Structural insights into the regulation of PDK1 by phosphoinositides and inositol phosphates. *EMBO J. 23*, 3918−3928.
(22) Knight, J. D., and Falke, J. J. (2009) Single-molecule fluorescence studies of a PH domain: New insights into the membrane docking reaction. *Biophys. J. 96*, 566−582.
(23) Ziemba, B. P., Knight, J. D., and Falke, J. J. (2012) Assembly of membrane-bound protein complexes: Detection and analysis by single molecule diffusion. *Biochemistry 51*, 1638−1647.
(24) Landgraf, K. E., Pilling, C., and Falke, J. J. (2008) Molecular mechanism of an oncogenic mutation that alters membrane targeting: Glu17Lys modifies the PIP lipid specificity of the AKT1 PH domain. *Biochemistry 47*, 12260−12269.
(25) Pilling, C., Landgraf, K. E., and Falke, J. J. (2011) The GRP1 PH domain, like the AKT1 PH domain, possesses a sentry glutamate residue essential for specific targeting to plasma membrane PI(3,4,5)-P_3. *Biochemistry 50*, 9845−9856.
(26) Yin, J., Lin, A. J., Golan, D. E., and Walsh, C. T. (2006) Site-specific protein labeling by Sfp phosphopantetheinyl transferase. *Nat. Protoc. 1*, 280−285.
(27) Knight, J. D., Lerner, M. G., Marcano-Velazquez, J. G., Pastor, R. W., and Falke, J. J. (2010) Single molecule diffusion of membrane-bound proteins: Window into lipid contacts and bilayer dynamics. *Biophys. J. 99*, 2879−2887.
(28) Corbin, J. A., Dirkx, R. A., and Falke, J. J. (2004) GRP1 pleckstrin homology domain: Activation parameters and novel search mechanism for rare target lipid. *Biochemistry 43*, 16161−16173.
(29) Goulian, M., and Simon, S. M. (2000) Tracking single proteins within cells. *Biophys. J. 79*, 2188−2198.
(30) Ziemba, B. P., and Falke, J. J. (2013) Lateral diffusion of peripheral membrane proteins on supported lipid bilayers is controlled by the additive frictional drags of 1) bound lipids and 2) protein domains penetrating into the bilayer hydrocarbon core. *Chem. Phys. Lipids*, DOI: 10.1016/j.chemphyslip.2013.04.005.
(31) Chen, H. C., Ziemba, B. P., Landgraf, K. E., Corbin, J. A., and Falke, J. J. (2012) Membrane docking geometry of GRP1 PH domain bound to a target lipid bilayer: An EPR site-directed spin-labeling and relaxation study. *PLoS One 7*, e33640.
(32) Lucas, N., and Cho, W. (2011) Phosphatidylserine binding is essential for plasma membrane recruitment and signaling function of 3-phosphoinositide-dependent kinase-1. *J. Biol. Chem. 286*, 41265−41272.
(33) Camley, B. A., and Brown, F. L. (2012) Contributions to membrane-embedded-protein diffusion beyond hydrodynamic theories. *Phys. Rev. E: Stat., Nonlinear, Soft Matter Phys. 85*, 061921.
(34) Landgraf, K. E., Malmberg, N. J., and Falke, J. J. (2008) Effect of PIP2 binding on the membrane docking geometry of PKCα C2 domain: An EPR site-directed spin-labeling and relaxation study. *Biochemistry 47*, 8301−8316.
(35) Lai, C. L., Landgraf, K. E., Voth, G. A., and Falke, J. J. (2010) Membrane docking geometry and target lipid stoichiometry of membrane-bound PKCα C2 domain: A combined molecular dynamics and experimental study. *J. Mol. Biol. 402*, 301−310.
(36) Biondi, R. M., Komander, D., Thomas, C. C., Lizcano, J. M., Deak, M., Alessi, D. R., and van Aalten, D. M. (2002) High resolution crystal structure of the human PDK1 catalytic domain defines the regulatory phosphopeptide docking site. *EMBO J. 21*, 4219−4228.